Available online at www.sciencedirect.com
SCIENCE DIRECT
Thermochimica Acta 440 (2006) 36–42
thermochimica acta
www.elsevier.com/locate/tca

Polyhedral oligomeric silsesquioxanes (POSS) thermal degradation

A. Fina [a,*,1], D. Tabuani [a,1], F. Carniato [b,1], A. Frache [a,1], E. Boccaleri [b,1], G. Camino [a,1]

[a] *Centro di Cultura per l'Ingegneria delle Materie Plastiche, Politecnico di Torino, V.le T. Michel 5, 15100 Alessandria, Italy*
[b] *Università del Piemonte Orientale, Dip. Scienze e Tecn. Avanzate, V. Bellini 25/G, 15100 Alessandria, Italy*

Received 28 June 2005; received in revised form 12 October 2005; accepted 12 October 2005
Available online 14 November 2005

Abstract

The mechanism of thermal degradation of several substituted polyhedral oligomeric silsesquioxanes (POSS) cages is studied in this work.

Hydrogen POSS and methyl POSS shows incomplete sublimation on heating, both in inert atmosphere and in air. Isobutyl and octyl substituted POSS undergo an almost complete evaporation when heated in inert atmosphere. In air, oxidation competes with volatilization, producing a considerable amount of silica-like residue on heating up to 800 °C.

Phenyl POSS shows a higher thermal stability than saturated aliphatic POSS and limited volatility, producing a ceramic residue at high yield on heating in nitrogen, composed of a silica containing a considerable amount of free-carbon. A lower amount of residue is shown after heating in air, corresponding to the POSS Si–O fraction.

A vinyl POSS cage/network resin is also studied, in comparison to above materials, showing the highest ceramic yield.

Keywords: POSS; Silsesquioxane; Thermal degradation

1. Introduction

Silsesquioxanes are compounds with general formula $(RSiO_{1,5})_n$, where R is an organic group or hydrogen [1–5], which attracted a wide research interest in the last years. Silsesquioxanes can have various geometrical structural orders, including random, ladder and cage structures; the latter are also known as polyhedral oligomeric silsesquioxanes (POSS). Compared to the others, they can be considered the smallest particles of organosilica currently available.

POSS are produced by sol–gel techniques through hydrolytic condensation of trifunctional monomers $RSiX_3$, X being a highly reactive substituent, such as Cl or alkoxy. Oligomeric silsesquioxanes were firstly synthesized in 1946 [6] and some research groups worked on POSS since 1960s [2,4] but only in the last decade several applications have been developed; this great interest arisen by POSS building blocks is mostly due to their hybrid organic/inorganic structure.

POSS were used for a variety of applications, from low dielectric constant materials to new resists for electron beam lithography materials and high temperature lubricants [7]. A further interest was given to POSS as their cage can easily be opened and further closed incorporating transition metals. These materials, featuring a geometrically well-defined catalytic centre, can be highly selective and active catalysts for organic reactions, both in homogeneous and heterogeneous catalysis, such as alkene polymerization, epoxydation and metathesis reactions [7–9].

Among the various applications of POSS, a very important field is the preparation of polymer nanocomposites and hybrids, with the aim to obtain multifunctional materials with intermediate properties between those of organic polymers and of ceramics.

In this field POSS were successfully used to improve polymer properties such as use temperature, oxidation resistance and mechanical properties; in some cases an interesting reduction of polymer flammability was reached [7,10,11].

In the light of this background, a deep insight on POSS thermal properties is necessary, in order to be able to tune the final properties of POSS-containing hybrids and nanocomposites.

Alkyl (from C_2 to C_{10}) substituted cubic cage POSS thermal properties were studied by Bolln et al. [12]; thermogravimetric analyses showed that, increasing the alkyl chain length, the

* Corresponding author. Tel.: +39 0131 229316; fax: +39 0131 229331.
E-mail address: alberto.fina@polial.polito.it (A. Fina).
[1] INSTM member.

0040-6031/$ – see front matter © 2005 Elsevier B.V. All rights reserved.
doi:10.1016/j.tca.2005.10.006

weight loss onset shifted to higher temperatures. Indeed, when heated in nitrogen (at 1 °C/min heating rate) these values ranged from 166 °C for octapropyl POSS to 355 °C for octadecyl POSS. Residues at the end of analysis were in the range between 5 and 15% of the initial weight and were believed by the authors to be due to a siloxane structure. Higher residual weights (from 30 to 50%) were found after heating POSS in air; the weight loss being higher with increasing alkyl chains length.

POSS degradation studies were also developed by Mantz et al. [13], who analysed gases (by means of FTIR and mass spectrometry) and chars from pyrolysis of both fully and partially condensed POSS. Fully condensed cyclohexyl trigonal prismatic and cubic POSS macromers [$R_6Si_6O_9$ and $R_8Si_8O_{12}$] were shown to have propensity to sublimation on heating in inert atmosphere. On the other end, the incompletely condensed POSS ($R_8Si_8O_{11}(OH)_2$) underwent a two-step degradation process, leading to a residue (40% of the initial weight) stable up to 1000 °C. In the first weight loss stage, sublimation was observed, together with traces of water and carbon dioxide in the degradation gases; these phenomena produced an insoluble residue, whose formation was explained through macromer's homopolymerization reactions occurring in competition with sublimation. In the second weight loss stage, evolution of cyclohexane and cyclohexene was observed due to the degradation of the first step residue.

Char analysis via solid-state ^{29}Si NMR and X-ray diffraction showed a progressive loss of cage structural order and crystalline structure, with increasing thermal treatment temperature.

In our previous work [14], the thermal degradation of octaisobutyl POSS was deeply studied: thermogravimetry showed evaporation of POSS leading to an almost complete weight loss independently on the heating rate, while in oxidising atmosphere an important residue at the end of treatment was obtained. The amount was found to be strongly related to the heating rate, ranging from 20% at 100 °C/min to 46% at 1 °C/min. The structure of residual solid phase after thermoxidative treatments was investigated by vibrational spectroscopy and X-ray diffraction, showing an organic amount decrease by increasing the treatment temperatures and a total conversion to amorphous silica by heating POSS up to 800 °C.

In a recent study, Zeng et al. reported the thermal degradation of octyl trisilanol POSS, during both programmed heating and isothermal conditions [15]. Heating octyl trisilanol POSS at 10 °C/min in nitrogen a single step weight loss (between 250 and 530 °C) was observed, leading to a 8% residue. When treated in isothermal conditions at 280 °C a viscous liquid was obtained, explained by silanol group condensation. Heating in air, a ceramic yield close to the theoretical value for conversion to silica was obtained; a similar amount (37%) of powdery residue was also reached in isothermal at 280 °C, explained by Si–C bonds cleavage and reorganisation in a solid structure.

Many literature reports are available on the thermal degradation of silsesquioxane homopolymers and copolymers; these materials are generally used as precursor for low dielectric materials (E&E sector) and for ceramics [3,16–19].

On the basis of this background, in this work we investigated the thermal and thermoxidative degradation of a series of fully condensed POSS in order to evaluate the effect of the chemical structure on the degradation pathway.

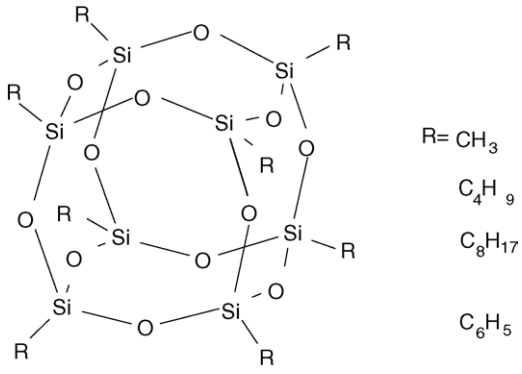

Fig. 1. T_8 POSS structure.

2. Experimental

The synthesis of octahydride POSS $H_8Si_8O_{12}$ (H-POSS) was carried on the basis of the Agaskar procedure [20]. The synthesis is an acid-catalysed hydrolytic condensation of $HSiCl_3$ (Sigma–Aldrich, reagent grade) carried on in a two-phase system based on a mixture of hexane/cyclohexane/toluene and acidic (HCl) water containing $FeCl_3$. This synthetic procedure led to the desired cubic cage (T_8) molecule, together with minor amounts of higher grade cages (T_{10} and T_{12}), as observed by GC–MS analysis.

Organic substituted POSS (Fig. 1) were obtained from Hybrid Plastics Company [21].

Methyl (me-POSS), isobutyl (ib-POSS) and "isoctyl" POSS[2] (io-POSS) were used as received. io-POSS is actually a cage mixture, containing T_8, T_{10} and T_{12} cages, as in the case of H-POSS; these products were not further purified because presence of different cages does not affect silsesquioxane thermal behaviour, as shown in this work.

Phenyl POSS (ph-POSS) was purified from residual solvents by drying in vacuum at 180 °C for 40 min. Since the commercial product was found to contain sodium chloride (observed by elemental analysis and X-ray diffraction), polyvinyl POSS (pv-POSS, Fig. 2) was purified by washing in deionised water and filtering on a 0.45 μm Millipore® polymeric membrane, then dried in vacuum at 80 °C for 2 h.

Thermogravimetry (TGA) was performed on a TA Q 500 instrument in platinum pans, with gas fluxes of 60 ml/min for sample gas (nitrogen or air) and 40 ml/min for balance protection gas (nitrogen).

Analyses were carried out in isothermal conditions or on heating at 10 °C/min, between 50 and 800 °C, on 10 mg samples.

High temperature TGA was performed on a Setaram SETSYS Evolution TGA, with 6 ml/min of argon protection gas and 14 ml/min sample gas (argon or air).

[2] Commercial "isoctyl POSS" R substituent is actually 2,2,4-trimethylpentyl, as stated by the producer.

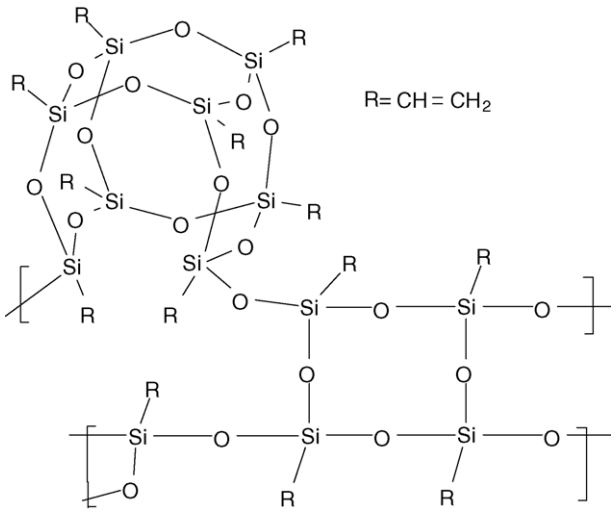

Fig. 2. Polyvinyl POSS (approximate structure [21]).

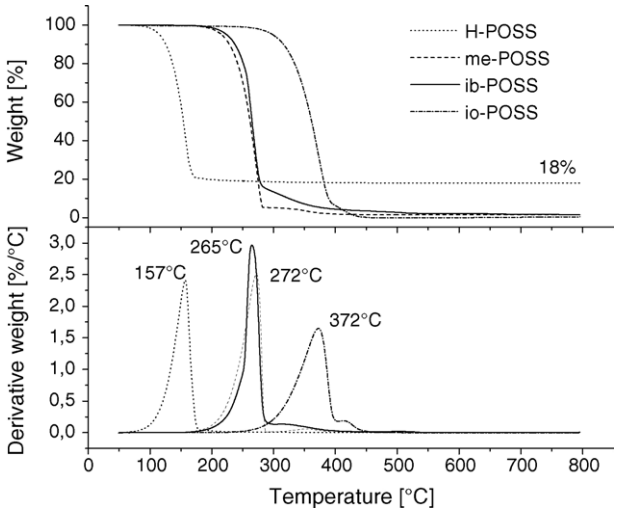

Fig. 3. Alkyl POSS TGA curves in nitrogen.

Differential scanning calorimetry (DSC) analyses were run using a Mettler DSC 30 instrument; measurements were done on 4 mg samples in open aluminium pans, under a nitrogen or air flow (30 ml/min). Heating rate was 10 °C/min.

Transmission FTIR spectra (resolution 4 cm^{-1}) were recorded on KBr pellets on a Perkin-Elmer Spectrum GXIII spectrophotometer. io-POSS, being a liquid at room temperature, was deposited on a monocrystalline silicon wafer.

Scanning electron microscopy (SEM) imaging was obtained by means of a LEO 1450 VP instrument.

Gas chromatography (GC) was performed on a Perkin-Elmer Autosystem XL, equipped with a medium polarity silica 30 m capillary column, coupled with a Perkin-Elmer Turbomass Gold Mass Spectrometer (MS). Flash pyrolyses in inert condition (He) were performed in a SGE Pyrojector Mk2 pyroliser, assembled on the GC injector (Py GC–MS).

3. Results and discussion

3.1. H- and alkyl POSS

The thermogravimetric curves in nitrogen for H-POSS and alkyl substituted POSS reported in Fig. 3 show a direct dependency of the weight loss temperature on the substituent type and size, both as regards onset and maximum weight loss rate temperature (T_{max}), which ranges from 157 °C for H-POSS to 372 °C for io-POSS.

The weight loss takes place in a single step and, except for H-POSS, it is almost complete, leaving a negligible amount of residue at 500 °C.

H-POSS thermal behaviour is explained by contemporary occurrence of sublimation above 100 °C, as reported by Calzaferri and Hoffman [22] and redistribution reactions [23,24], leading to a silica residue.

The degradation processes of alkyl-POSS have been ascribed to a volatilization phenomenon influenced by the substituent size: me-POSS was recognized to undergo almost complete sublimation [4,25], while longer chain POSS evaporate above melting temperature [14,12].

In air the behaviour on heating may be very different from what observed in inert atmosphere, as oxygen plays an active role in the degradation process. Indeed, the two longer alkyl-chain POSS (ib- and io-POSS) show a considerable amount of colourless glassy residue at 800 °C. The initial weight loss for ib-POSS occurs at a temperature close to that observed in inert atmosphere (ca. 200 °C) but the evaporation is incomplete (Fig. 4). io-POSS weight curve shows a two-step oxidation of octyl groups, at temperatures lower than that necessary for POSS evaporation. This behaviour prevents evaporation and leads to a residue amounting to 27% of the initial weight, which is close to the io-POSS inorganic fraction amount (31%).

The proposed mechanism for the POSS bearing longer alkyl chains involves the competition between the evaporation process already observed in nitrogen and an oxidation phenomenon, which leads to a thermally stable residue. This oxidation mechanism involves the peroxidation of the alkyl chains and the subsequent fragmentation through classical radical pathways [14].

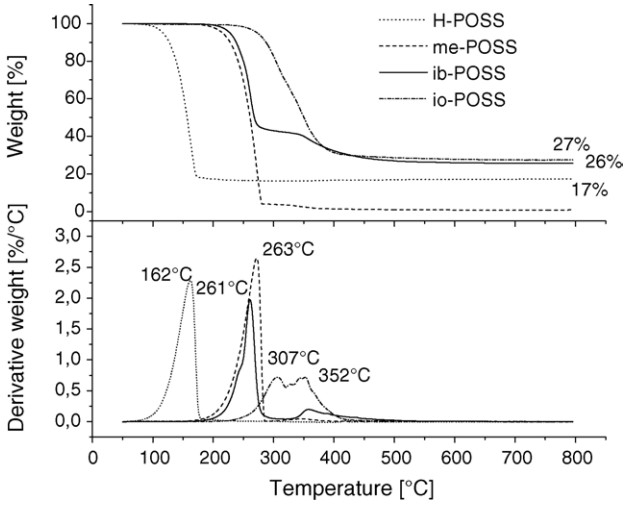

Fig. 4. Alkyl POSS TGA curves in air.

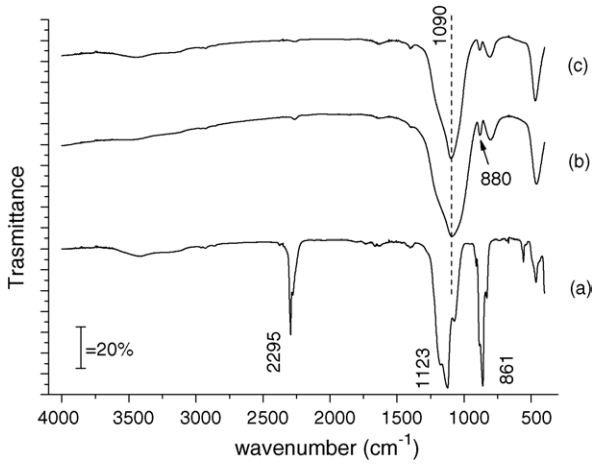

Fig. 5. FTIR spectra for H-POSS heated in different conditions: (a) room temperature, (b) heated to 800 °C in N_2, (c) heated to 800 °C in air.

The weight loss curves in air for H-POSS and me-POSS are very similar to those obtained in nitrogen both as regards the degradation temperature and as regards the residual weight, indicating that the effect of oxygen on their degradation patterns is negligible. In the case of me-POSS, this is probably due to the lower reactivity towards oxygen of the primary carbon atom as compared to ib- and io-POSS, while the proposed mechanism for H-POSS thermal degradation involves SiH_4 oxidation in gas phase [24].

The residues obtained from the thermal treatments have been studied by means of FTIR spectroscopy, in order to investigate the evolution of the chemical structure during heating.

In Fig. 5 the spectra of H-POSS and of the residues after heating at 800 °C in nitrogen and in air are shown. H-POSS spectrum (a) clearly shows signals from Si–O stretching (ca. 1123 cm^{-1}), Si–H stretching (ca. 2295 cm^{-1}) and bending (ca. 861 cm^{-1}), partially splitted because of solid-state effects on molecular symmetry, in agreement with what previously reported [26,27]. The spectra of the residues (b) and (c) show some weak residual Si–H bending signal (880 cm^{-1}) and the broad band from Si–O bonds stretching. Moreover, the centre of the absorption band for Si–O is shifted to lower wavenumbers (ca. 1090 cm^{-1} versus 1123 cm^{-1}); these results can be related to the formation of inter-cage stretched Si–O bonds, in agreement with previous studies [16,17].

In our previous work [14], the residues obtained after thermal treatments of ib-POSS in air were studied in detail by FTIR and Raman spectroscopies. The characteristic signals for the organic fraction (in particular the C–H stretching bands around 2900 cm^{-1}) were found to decrease by increasing the treatment temperature, showing the progressive loss of POSS organic fraction. In parallel, absorptions of Si–O bonds stretching modes for the 200 and 300 °C residues occurred at lower wavenumbers with respect to pristine ib-POSS. This behaviour is in accordance with what observed here for H-POSS, indicating the formation of a Si–O–Si network structure. After heating to 800 °C, the infrared spectrum was totally consistent with that of an amorphous silica.

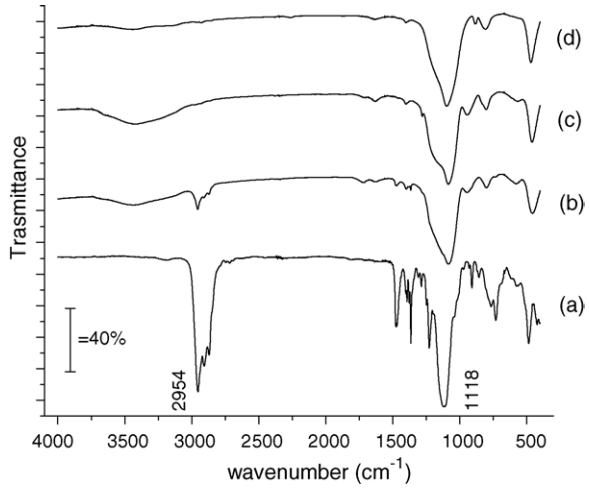

Fig. 6. FTIR spectra for io-POSS heated in air at increasing temperatures. (a) Room temperature; (b) treated 250 °C, 2 h; (c) treated 350 °C, 1 h; (d) heated to 800 °C, 10 °C/min.

A similar behaviour on heating in air is observed with io-POSS (Fig. 6); the signals related to the organic fraction (around 2900 cm^{-1}) are strongly reduced after treatment at 250 °C, and are almost completely lost after heating up to 350 °C. Once again, the spectrum for io-POSS heated up to 800 °C is very close to that of SiO_2.

3.2. Phenyl POSS

The thermal behaviour of ph-POSS is completely different from those of alkyl substituted POSS (Fig. 7); this kind of POSS, in fact, is thermally stable up to 350 °C and produces a considerably higher residue with respect to alkyl-POSS both in nitrogen and in air.

In nitrogen, a two-step weight loss is observed, with maximum rates at 466 and 623 °C, producing a 70% stable black glass residue at 700 °C. The POSS volatilization effect observed

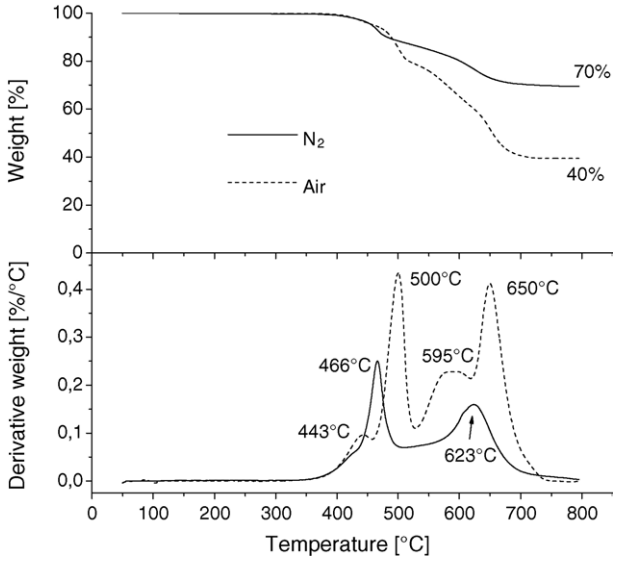

Fig. 7. ph-POSS TGA curves.

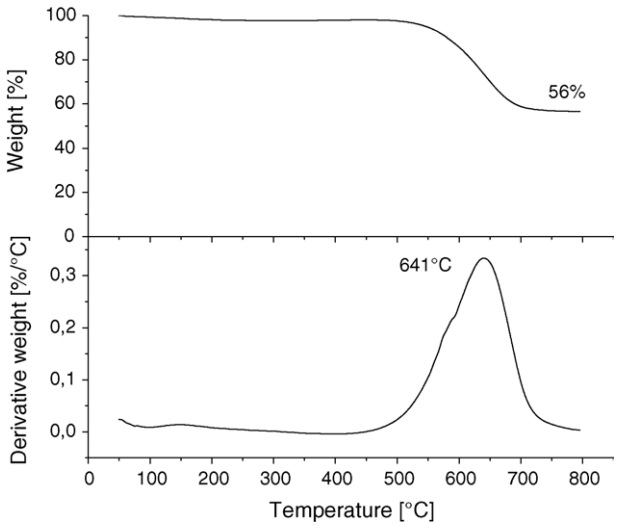

Fig. 8. TGA curve in air for nitrogen-obtained ph-POSS residue.

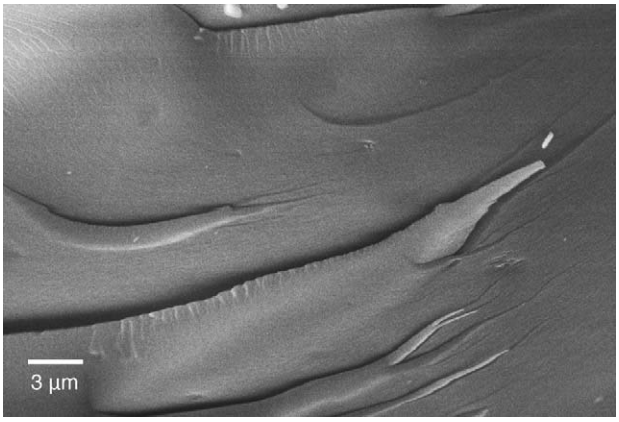

Fig. 9. SEM micrography showing N2-obtained ph-POSS residue morphology (7000×).

with alkyl POSS is probably here in competition with chemical reactions, due to the higher melting temperature of ph-POSS (500 °C; [28]). The higher residue percentage, with respect to inorganic Si–O fraction in ph-POSS (ca. 40%) can be attributed to the entrapment of carbon in the structure, probably due to phenyl group condensation.

In air a similar behaviour is shown, with two main weight loss steps (500 and 650 °C), accompanied by two minor phenomena at lower temperatures (443 and 595 °C). The almost colourless residue after treatment is ca. 40% of the initial weight and can be accounted for by the quantitative oxidative transformation of POSS to silica.

Preliminary study of volatile products by Py GC–MS shows benzene release; a complete study of gaseous degradation products will be the matter of further studies. In order to check the thermoxidative stability of the nitrogen-atmosphere residue, the material was ground into powder and re-heated up to 800 °C in air (Fig. 8). The results show a single weight loss step, starting over 400 °C, with a maximum rate at 641 °C, leading to 56% of an almost white powder.

The amount (56% of 70% equals 39%) and visual aspect of this material is very close to the one obtained by direct heating of ph-POSS in air. This fact confirms the presence of free carbon in the structure that undergoes oxidation during the treatment in air.

The carbonaceous moieties present in the sample are not aggregated, but are homogenously dispersed in the material: indeed, SEM analysis on the residue obtained after heating to 800 °C in nitrogen does not show any microscopic phase separation (Fig. 9).

The FTIR analyses on ph-POSS residues are shown in Fig. 10. The ph-POSS IR spectrum (a) shows signals for Si–O framework (band around 1100 cm^{-1}) together with signals from the organic fraction: peaks at 697 and 746 cm^{-1} are related to phenyl groups out-of-plane deformation, signals at 1137 cm^{-1} (partially overlapped with Si–O band) and 1432 $cm^{-1}$are due to Si-phenyl group bonds deformation; C=C bonds stretching is shown by peak at 1595 cm^{-1} [29], while bands around 3000 cm^{-1} are attributed to C–H bonds stretching modes. In particular, signals in the range 3000–3100 cm^{-1} are relative to C–H on phenyl groups, while the ones at 2850–3000 cm^{-1} are probably related to residual solvent in ph-POSS (see Section 2).

The spectrum for the residue obtained in air is fully consistent with silica structure, while the nitrogen residue shows an additional band centred at ca. 1600 cm^{-1} (see inset Fig. 10), partially overlapped with the water molecules bending deformation at 1630 cm^{-1}. This signal is probably related to C=C bonds stretching and it confirms the presence of free carbon in the residue structure [30,31].

3.3. Polyvinyl silsesquioxane

A different thermal behaviour from above POSS is shown by the cured polyvinyl silsesquioxane.

In inert atmosphere, two weak weight losses are observed, followed by a more significant one, starting above 450 °C, leading to a final 93 wt.% thermally stable residue at 800 °C (Fig. 11a).

The DSC curve (Fig. 11b) shows an exothermic process starting above 200 °C with maximum heat flow at about 480 °C. This phenomenon can be related to the occurrence of vinyl

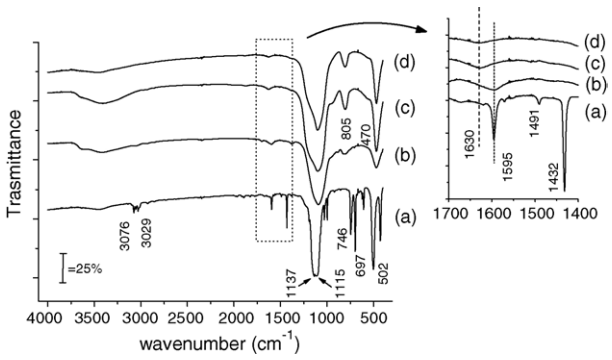

Fig. 10. FTIR spectra for ph-POSS residues. (a) Room temperature; (b) heated to 800 °C, 10 °C/min in N_2; (c) heated to 800 °C, 10 °C/min in air; (d) heated to 800 °C, 10 °C/min in N_2, then 800 °C, 10 °C/min in air.

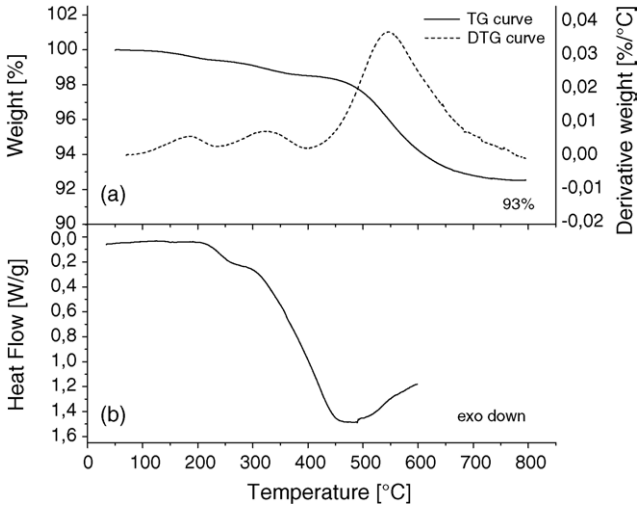

Fig. 11. pv-POSS TGA (a) and DSC (b) curves in nitrogen.

groups polymerization, that leads to further POSS crosslinking, with the formation of a continuous –O–Si–C_n–Si–O structure. Increasing temperature above 400 °C, both C–C and Si–C bonds can be partially cleaved, with production of volatiles explaining the observed main weight loss. In order to identify the degradation products, pyrolyses at 600 °C were performed and the volatiles were analysed by GC–MS analysis, showing the release of alkenes with chain length from C_2 to C_{15}. This is explained by the detachment of unreacted (due to steric hindrance) vinyl groups and by the partial elimination of longer chains formed during the POSS organic chains polymerization.

In air above 170 °C the POSS resin increases its weight up, in analogy with what reported by Voronkov and Lavrent'yev for octavinyl POSS [4]; the maximum weight gain was about 6%: above 260 °C, a continuous weight loss occurs (Fig. 12a). At 800 °C a residue equal to 80% of the initial weight is left. At this temperature, DTG curve slightly greater than 0 shows that

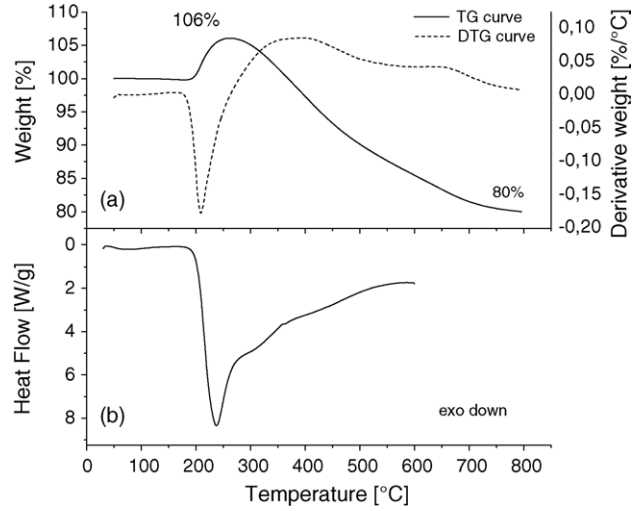

Fig. 12. pv-POSS TGA (a) and DSC (b) curves in air.

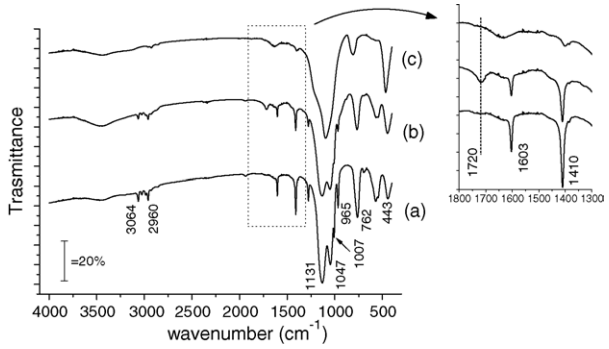

Fig. 13. FTIR spectra for pv-POSS heated in air. (a) Polyvinyl POSS at room temperature; (b) heated to 250 °C, 10 °C/min; (c) heated to 800 °C, 10 °C/min.

the residue is still not completely stable; heating pv-POSS to higher temperatures (1500 °C, 10 °C/min) a 78% stable residue is obtained, for temperatures above 1200 °C.

Thermogravimetric analysis performed in isothermal conditions at 200 °C showed an 8 wt.% gain that levels off after 40 min.

The DSC curve in air (Fig. 12b) enabled us to understand the thermo-oxidation mechanism showing a strong exothermic signal above 200 °C, probably due to organic fraction peroxidation overlapping with vinyl polymerization. Peroxidation explains the observed weight gain; indeed FTIR analysis after heating to 250 °C (Fig. 13b) shows the appearance of an absorption peak centred at 1720 cm^{-1} (see inset Fig. 13), corresponding to the stretching of C=O bonds derived from oxidation of part of the organic groups. The contemporary presence of both C=O band and signals for vinyl groups (C=C stretching at 1603 cm^{-1}, CH_2 deformation at 1410 cm^{-1}, CH wagging at 1007 cm^{-1}, CH_2 wagging at 965 cm^{-1}) indicates that only a part of the organic groups can be oxidized. IR spectrum of 200 °C isothermally treated pv-POSS shows very similar results.

Above 400 °C, the high efficiency of organic chains elimination due to the oxidation process, leads to a residue which is lower than that obtained after heating in nitrogen. After heating to 800 °C (Fig. 13c), contemporarily with the loss of the main signals related to the organic substituents, the two bands centred at 1131 and 1047 cm^{-1} due to cage and network Si–O bonds stretching are broadened to a single, unresolved band, showing a more disordered silica-like structure, as already observed with the other POSS object of this study.

Considering that the inorganic Si–O fraction in pv-POSS is about 65% of the total weight, the higher residues after both treatments in nitrogen (93%) and in air (80%) evidences the presence of carbon in the structure. Both residues obtained on heating in nitrogen and in air appear dark. Moreover, when the residue obtained at 800 °C in nitrogen is re-heated in air, a further weight loss occurs, leading to the same ceramic amount obtained after heating in air, showing the presence of a small amount of carbonaceous phase, in analogy with what reported for ph-POSS.

Differently from what observed for ph-POSS, here a carbon-containing phase is likely formed even after treatment in air.

4. Conclusions

Thermal and thermoxidative behaviours are shown to depend on POSS type of substitution. Alkyl-substituted POSS showed evaporation or sublimation in inert atmosphere, over a range of temperature dependent on POSS molecular weight, ranging from ca. 100 °C for H-POSS to 300 °C for io-POSS. In air, oxidation takes place on the organic chains and leads to a cage crosslinking, producing a ceramic silica-like phase.

Phenyl POSS showed a higher thermal stability and did not undergo significant volatilization. After heating in nitrogen, ceramic yield is much higher than for alkyl-POSS; this residue contains a fraction of free carbon, produced by phenyl groups condensation. When heated in air, the whole organic fraction is oxidized and a silica-like phase is obtained, in amounts close to the POSS inorganic fraction.

The differences observed between alkyl T_8 POSS and phenyl T_8 POSS is due to the organic groups intrinsic stability, which results in differences in their degradation pathways. Considering behaviour in nitrogen, POSS alkyl chain could form volatiles both by Si–C cleavage and carbon–carbon chain cracking, producing unsaturated moieties [14]. On the other end, the only possible mechanism to evolve benzene from phenyl POSS is by hydrogen abstraction from phenyl groups; thus, the resulting aromatic radicals could combine creating a very stable polyaromatic structure. When heating in air, oxidation reactions take place in both cases, progressively consuming all carbon (either aliphatic or aromatic) from the solid phase.

The study of a polyvinyl POSS, in comparison with the previous ones, evidenced the highest ceramic yield, through the material reorganization into a O–Si–C_n–Si structure. During heating in inert atmosphere this process involves the POSS crosslinking through vinyl groups polymerization, followed by partial organic fraction elimination and production of a small amount of carbonaceous phase. In air, a similar pathway is observed, accelerated by oxygen presence.

As ceramics could be exploited in protection for macromolecular materials towards high temperature, an interesting application for POSS is in fire retardancy of polymeric materials. In a polymer nanocomposite, POSS could evolve to a ceramic superficial layer during the earlier stage of combustion, protecting the underlying material by limiting heat transfer as well as hampering diffusion of oxygen and evacuation of combustible products, in analogy with layered silicates [32].

Acknowledgements

This study was carried out in the frame STRP European research program “NANOFIRE”, no. 505637, in the sixth Framework Program.

References

[1] G. Li, L. Wang, H. Ni, C.U. Pittman Jr., J. Inorg. Organomet. Polym. 11 (2001) 123–154.
[2] P.G. Harrison, J. Organomet. Chem. 542 (1997) 141–183.
[3] R.H. Baney, M. Itoh, A. Sakakibara, T. Suzuki, Chem. Rev. 95 (1995) 1409–1430.
[4] M.G. Voronkov, V.I. Lavrent’yev, Top. Curr. Chem. 102 (1982) 199–236.
[5] K.J. Shea, D.A. Loy, Chem. Mater. 13 (2001) 3306–3319.
[6] D.W. Scott, J. Am. Chem. Soc. 68 (1946) 356–358.
[7] Proceedings of POSS Nanotechnology Conference, Huntington Beach, CA, September, 2002.
[8] H.C.L. Abbenhuis, Chem. Eur. J. 6 (2000) 25–32.
[9] http://www.hybridcatalysis.com.
[10] J.D. Lichtenhan, J.W. Gilman, US Patent 6,362,279 (2002).
[11] S. Lu, I. Hamerton, Prog. Polym. Sci. 27 (2002) 1661–1712.
[12] C. Bolln, A. Tsuchida, H. Frey, R. Mülhaupt, Chem. Mater. 9 (1997) 1475–1479.
[13] R.A. Mantz, P.F. Jones, K.P. Chaffee, J.D. Lichtenhan, J.W. Gilman, Chem. Mater. 8 (1996) 1250–1259.
[14] A. Fina, D. Tabuani, A. Frache, E. Boccaleri, G. Camino, in: M. Le Bras, C. Wilkie, S. Bourbigot (Eds.), Fire Retardancy of Polymers: New Applications of Mineral Fillers, Royal Society of Chemistry, Cambridge, UK, 2005, pp. 202–220.
[15] J. Zeng, C. Bennett, W.L. Jarrett, S. Iyer, S. Kumar, L.J. Mathias, D.A. Schiraldi, Compos. Interfaces 11 (2005) 673–685.
[16] M.J. Loboda, C.M. Grove, F. Schneider, J. Electrochem. Soc. 145 (1998) 2861–2866.
[17] M.G. Albrecht, C. Blachette, J. Electrochem. Soc. 145 (1998) 4019–4025.
[18] H. Zhang, C.G. Pantano, J. Am. Ceram. Soc. 73 (1990) 958–963.
[19] F.I. Hurwitz, P. Heimann, S.C. Farmer, D.M. Hembree, J. Mater. Sci. 28 (1993) 6622–6630.
[20] P.A. Agaskar, Inorg. Chem. 30 (1991) 2707–2708.
[21] Structures reported on the hybrid plastics catalog at http://www.hybridplastics.com.
[22] G. Calzaferri, R. Hoffmann, J. Chem. Soc., Dalton Trans. (1991) 917–928.
[23] V. Belot, R.J.P. Corriu, D. Leclercq, P.H. Mutin, A. Vioux, J. Mater. Sci. Lett. 9 (1990) 1052–1054.
[24] V. Belot, R. Corriu, D. Leclercq, P.H. Mutin, A. Vioux, Chem. Mater. 3 (1991) 127–131.
[25] L.H. Vogt, J.F. Brown, Inorg. Chem. 2 (1963) 189–192.
[26] P. Bornhauser, G. Calzaferri, Spectrochim. Acta, Part A 46 (1990) 1045–1056.
[27] A.D. Chomel, U.A. Jayasooriya, F. Babonneau, Spectrochim. Acta, Part A 60 (2004) 1609–1616.
[28] J.F. Brown, L.H. Vogt, P.I. Prescott, J. Am. Chem. Soc. 86 (1964) 1120–1125.
[29] D. Lin-Vien, N.B. Colthup, W.G. Fateley, J.G. Grasselli, The Handbook of Infrared and Raman Characteristics Frequency of Organic Molecules, Academic Press Inc., San Diego, CA, 1991.
[30] P.C. Eklund, J.M. Golden, R.A. Jishi, Carbon 33 (1995) 959–972.
[31] A. Galvez, N. Herlin-Boime, C. Reynaud, C. Clinard, J.N. Rouzaud, Carbon 40 (2002) 2775–2789.
[32] M. Zanetti, T. Kashiwagi, L. Falqui, G. Camino, Chem. Mat. 14 (2002) 881–887.